V International Conference on Computational Methods for Coupled Problems in Science and Engineering
COUPLED PROBLEMS 2013
S. Idelsohn, M. Papadrakakis and B. Schrefler (Eds)

MODAL CHARACTERISTICS OF A FLEXIBLE TUBE IN TURBULENT AXIAL FLOW: A NUMERICAL APPROACH AND VALIDATION WITH EXPERIMENTAL DATA

J. DE RIDDER*, J. DEGROOTE*, K. VAN TICHELEN†, P. SCHUURMANS† AND J. VIERENDEELS*

*Department of Flow, Heat and Combustion Mechanics
Ghent University
Sint-Pietersnieuwstraat 41, 9000 Ghent, Belgium
e-mail: j.deridder@ugent.be, joris.degroote@ugent.be, jan.vierendeels@ugent.be - web page: http://www.ugent.be/ea/floheacom/en/

†Belgian Nuclear Research Center
Boeretang 200, 2400 Mol, Belgium
e-mail: kvtichel@sckcen.be, pschuurm@sckcen.be - web page: http://www.sckcen.be/

Key words: flow-induced vibration, modal characteristics, turbulent axial flow, numerical method

Abstract. Flow-induced vibration is an important concern in the design of tube bundles. Due to the coupling of fluid motion and structural motion, instabilities such as flutter and divergence can arise. Next to the instabilities caused by the coupling of fluid motion and structural motion, turbulence could cause small amplitude vibrations, which in turn could give rise to long-term damage. Currently, the dynamical behavior of a tube in axial flow is studied by splitting the flow forces into inviscid and viscous components. The inviscid flow forces are determined from potential flow theory while the viscous flow forces come from empirical formulations.

In this paper, a computational methodology is proposed to improve the accuracy of the predicted dynamical behaviour. In this methodology partitioned fluid-structure interaction simulations are performed to calculate the free vibration decay of a tube in axial flow. The tube is initially deformed according to an eigenmode in vacuum. Modal characteristics are then derived from the free vibration decay of the tube surrounded by the turbulent water flow. To validate this computational methodology a series of experiments is reproduced. In these experiments the frequency and damping of the fundamental mode of a solid brass cylinder were measured.

1 INTRODUCTION

Flow-induced vibration is an important concern in the design of tube bundles, both in axial-flow as well as cross-flow configurations. Applications with an axial-flow regime are typically found in nuclear reactors while cross-flow regimes are typically found in shell-and-tube heat exchangers. This article will focus on axial flow.

Different types of flow-induced instabilities can arise in tube bundles subjected to axial flow, depending on their fixations. Generally however, due to the coupled fluid-structure motion, centrifugal fluid forces can trigger a static instability while Coriolis forces can trigger a dynamic one [1]. Next to the instabilities caused by the coupled motion, small vibrations are triggered by turbulent fluctuations in the flow. While these vibrations are not as catastrophic as the ones induced by the coupled fluid-structure motion, they can damage the structure in the long term.

In order to predict the vibrational behavior of a tube exposed to axial flow, classical models split the flow forces induced by the motion into an inviscid part and a viscous part [2]. The inviscid forces can be derived from potential flow theory. They result in a force proportional to the acceleration (an added mass), a centrifugal force and a Coriolis force. The viscous (turbulent) forces are based on a linearization of empirically determined turbulent friction forces. Research on the constants required in these expressions is still on-going [3]. In cross-flow configurations some authors use (2D) CFD-simulations to establish the required coefficients [4].

Research based on CFD is mainly concerned with cross-flow regimes, in which vortex shedding is one of the important mechanisms of flow-induced vibration. Regarding axial flow a solver was developed for instabilities in laminar flow conditions and later a linearized solver for turbulent annular flow configurations was developed. The initial solver was based on a staggered approach. To keep the computation stable with higher added fluid masses, an estimation of the added mass was afterwards included in the structural solver [5].

In this paper, modal characteristics of a tube in turbulent water flow will be computed directly from coupled computational fluid mechanics (CFD) and computational solid mechanics (CSM). To assess the accuracy of the proposed methodology, the results are compared to experimental results available in open literature.

2 METHODOLOGY

Essentially, modal characteristics in this paper are determined from unsteady computations of the free decay of initially deformed structures [6]. The computations are split into four steps:

STEP 1: Computation of eigenmodes in vacuum

Initially the eigenmodes in vacuum are computed with a finite element solver, searching eigenmodes of:

$$(K - M\omega^2)x_i = 0 \tag{1}$$

with K the stiffness matrix, M the mass matrix and x_i the displacements.
STEP 2: Initialization of the fluid-structure interaction (FSI) simulation
The cylinder is then deformed according to the previously determined fundamental mode shape. The steady-state flow around the deformed cylinder is computed, thus solving the steady-state mass balance and Navier-Stokes equations for an incompressible fluid:

$$\nabla \cdot v_f = 0 \tag{2}$$

$$\rho_f \left(v_f \cdot \nabla v_f\right) = -\nabla p + \mu_f \nabla \cdot \nabla v_f + f_f \tag{3}$$

in which p stands for pressure, v_f for fluid velocity, ρ_f for fluid density, μ_f for fluid viscosity.
STEP 3: Unsteady FSI-calculation
The deformed structure and the flow field serve as initial state in an unsteady FSI-simulation. In this simulation both the kinematic and dynamic equations need to be satisfied:

$$d_s = d_f \tag{4}$$

$$-\tau_s \cdot n_s = \tau_f \cdot n_f \tag{5}$$

with d_s, d_f the displacement of the interface on the structural side and on the fluid side respectively, τ_f, τ_s the stress on the interface due to the fluid and due to the structure and n_s, n_f the surface normals on the fluid-structure interface of the structural and the fluid domain. The Newtonian fluid flow itself is governed by the incompressible form of the conservation of mass and the Navier-Stokes equations:

$$\nabla \cdot v_f = 0 \tag{6}$$

$$\rho_f \left(\frac{\partial v_f}{\partial t} + v_f \cdot \nabla v_f\right) = -\nabla p + \mu_f \nabla \cdot \nabla v_f \tag{7}$$

The structural displacement is governed by Newton's second law:

$$\rho_s \frac{\partial^2 d_s}{\partial t^2} = \nabla \cdot \tau_s \tag{8}$$

with ρ_s the solid density, τ_s the stress tensor, which is determined using the constitutive equation of the material.
STEP 4: Extraction of the modal characteristics
From the previous step the free vibration decay in a fluid of the original in vacuum mode is available. This vibration can be developed into series of N decaying modes:

$$d_{cl,i}(z,t) \approx d_{cl,i,est}(z,t) = \sum_{i=1}^{N} a_i(z) \exp(-2\pi f_i \zeta_i t) \sin(2\pi \sqrt{1-\zeta_i^2} f_i t + \theta_i) \tag{9}$$

with $a_i(z)$ the mode shape, ζ_i the modal damping ratio, f_i the frequency and θ_i the phase angle of mode i.

3 SIMULATION DETAILS

The geometry computed in this paper is based on the geometry described in [7]. It consists of a solid brass cylinder mounted in a water-conveying pipe. The geometrical parameters as well as material properties are listed in Table 1. The cylinder was pre-tensioned with 648 N. In the experiments the water speed ranged from 10 m/s to 30 m/s.

Table 1: Geometrical parameters and material properties

Geometrical parameters	
cylinder diameter	0.0127 m
cylinder length	1.19 m
hydraulic diameter	0.0127 m
Material properties	
density of brass	8400 kg/m^3
Young's modulus of brass	107 GPa
Poisson's ratio of brass	0.34
water density	1000 kg/m^3
water viscosity	0.001 $Pa.s$

The flow is thus turbulent with Reynolds numbers between 124000 and 372000. It is computed by solving URANS-equations, with the $k-\omega$ SST model. The influence of different inlet turbulent intensities is studied. As the cylinder is moving, the flow equations are cast in the ALE (arbitrary Lagrangian-Eulerian) form. The mesh motion is computed by iteratively solving a system of springs. The flow solver uses a 2nd-order discretization, both in space and in time.
The CSM-calculation is a finite element calculation, which uses 2nd-order elements and the Hilber-Hughes-Taylor time-integrator, which is also of 2nd-order accuracy. The fluid-structure coupling is computed with the IQN-ILS algorithm [8].

4 CONVERGENCE STUDY

4.1 Number of modes required in the free-vibration fitting

In the case, studied in this article, the mode shapes of the coupled fluid-structure are very similar to ones of the pure structural problem. As a result, only one mode is required to predict the decay of the fundamental mode. Fitting with one mode already gave R^2-values of more than 99.9%.
The goodness of fit can also be seen on Figure 1, which plots the reconstructed displacement as a function of time, together with the error to the original displacement. The error graph shows peaks probably belonging to a small 2nd-mode contribution.

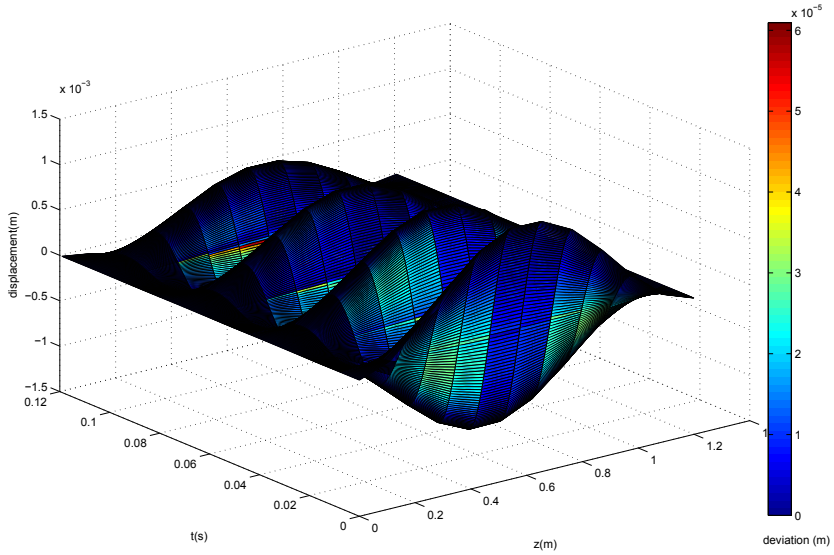

Figure 1: Reconstructed displacements in function of time and axial coordinate, colored by the error to the original signal

4.2 Influence of time step size

If the time step in the simulations is chosen too large, the modal damping ratio is typically overestimated [6]. However, in the case studied here, neither the modal damping ratio nor the natural frequency were very sensitive to the time step size, as can be seen in Figure 2. In the remainder of the article a time step size of 0.2 ms is used, as it reduces the computational cost.

4.3 Grid convergence

The grid used for the finite-element calculation consists of 400 quadratic 3D-elements. Grid refinements showed no significant change in eigenmodes or eigenvalues.
The mesh used in the CFD-calculation consists of 235000 cells. The first grid point is located in the logarithmic region, as its y^+-value is 200 for a water velocity of 30 m/s. Modal characteristics were also determined with a mesh consisting of only 62500 cells. Neither the frequency nor the damping showed appreciable difference with the mesh normally used.

5 RESULTS

In this section the influence of inlet conditions, water velocity and molecular viscosity is discussed.

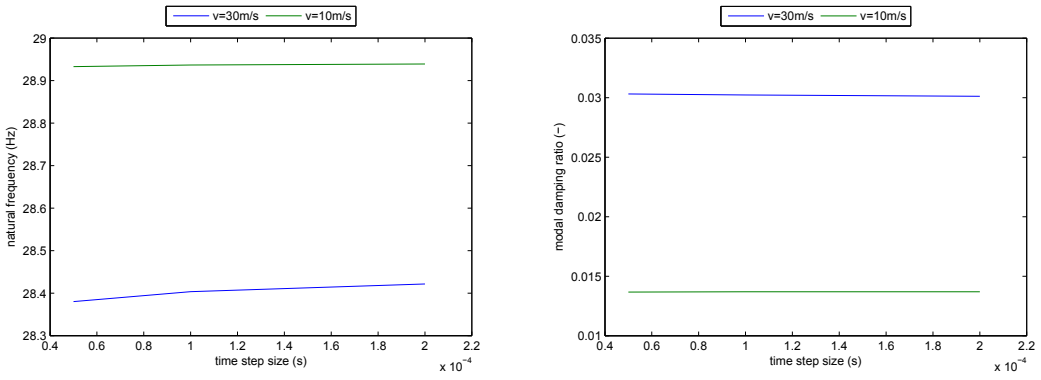

Figure 2: Influence of the time step size on the natural frequency (left graph) and the modal damping ratio (right graph)

5.1 Influence of inlet conditions

In order to solve the (U)RANS-equations, two additional turbulent quantities are required at the inlet. They will alter the turbulent (eddy) viscosity downstream, which influences the modal damping.
As the ratio of the channel length over its hydraulic diameter (Dh) is relatively high, the flow becomes already fully developed at the beginning of the channel. From Figure 5.1, the flow is fully developed after approximately 20 Dh, while the entire channel length is approximately 95 Dh. Changes in inlet turbulence characteristics only modifies the turbulent viscosity in the beginning of the channel. This is in agreement with experimental work performed by Mulcahy [9].
These changes in turbulent viscosity do not result in significant changes of modal characteristics (on the order of 1 %), as they are only occurring in a limited part of the domain and the modal shape is very small in that part.

5.2 Influence of water velocity

If the flow velocity is high enough, divergence or flutter of the cylinder could occur. Conventional theories predicting flow-induced vibration often recast the flow velocity in a dimensionless form [2]:

$$v_{f,n} = \left(\frac{EI}{\rho_f A}\right)^{-0.5} v_f L \tag{10}$$

with I the second moment of inertia and E the Young's modulus of elasticity. For a flow velocity of 30 m/s this dimensionless flow velocity is still only 1.1. Flow instabilities typically occur for non-dimensional flow velocities greater than 2-6 [2].
While the flow velocity is not high enough to trigger flow-induced instabilities, it does change the modal characteristics, as can be seen in Table 2. An increase of flow velocity leads to lower natural frequencies and higher modal damping ratios. The decrease in

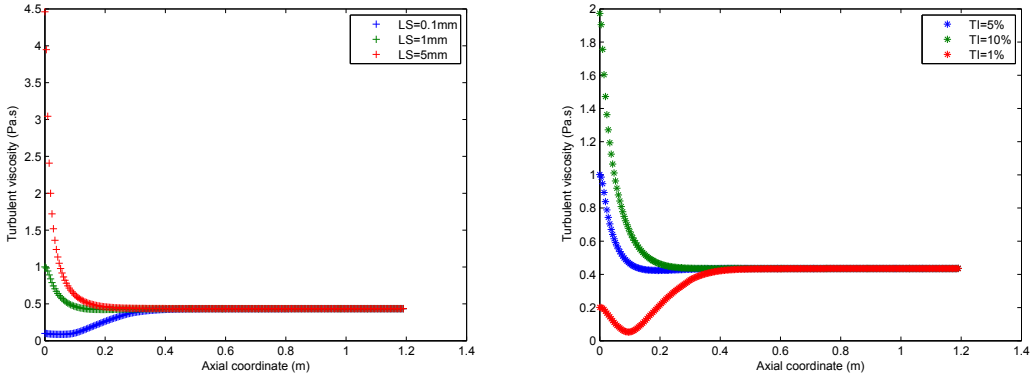

Figure 3: Influence of the inlet turbulence length scale (left graph) and turbulence intensity (right graph) on the turbulent viscosity at $Dh/8$ from the cylinder

Table 2: Natural frequency and modal damping ratio of the ground mode vibration as a function of flow velocity

	computed values		experimental values [7]	
v_f (m/s)	f_n (s^{-1})	ζ_n $(-)$	f_n (s^{-1})	ζ_n $(-)$
10	28.9	0.014	27.9	0.013
20	28.7	0.022	27.7	0.021
30	28.4	0.030	27.5	0.030

natural frequency can be explained by an increase of centrifugal forces acting on the cylinder, while the increase in modal damping can be attributed to the increase of turbulent viscosity. Table 2 further shows a good agreement between the computed characteristics and the experimentally determined characteristics.
While current theories have similar reliability on frequency prediction compared to the calculations in this article, they have to include an empirical friction correlation to predict the modal damping ratio.

5.3 Influence of molecular viscosity

The molecular viscosity is not exactly known as the water temperature is not well known. Therefore, different computations with a molecular viscosity between 0.0005 Pa.s and 0.002 Pa.s have been carried out.
For a flow velocity of 30 m/s, the turbulent viscosity is 431 times the molecular one. The molecular viscosity will thus only affect the modal characteristics because it alters its turbulent counterpart.
Table 3 lists the modal characteristics and the average turbulent viscosity for different molecular viscosities. The molecular viscosity has almost no influence on the natural

Table 3: Modal characteristics for different molecular viscosities

$\mu_f(Pa.s)$	f_n (s^{-1})	ζ_n $(-)$	$\mu_t(Pa.s)$
0.0005	28.4	0.0281	0.412
0.001	28.4	0.0303	0.431
0.002	28.3	0.0331	0.450

frequency. However, it influences the modal damping ratio, through changes in turbulent viscosity.

6 CONCLUSION

Modal characteristics are computed purely numerically in this article. It has the advantage over conventional methods that it does not require specific empirical input. The results obtained with the method, presented in this article, have been compared and validated with experiments available in open literature.
The calculations showed that the influence of inlet conditions decayed after 20 Dh. This observation is in accordance with experimental findings. An increase in flow speed gave slightly lower frequencies and significant higher modal damping ratios. Changes in molecular viscosity resulted in slightly different turbulent viscosities and thus slightly different modal damping ratios.

REFERENCES

[1] S. Chen, *Flow-induced vibration of circular cylindrical structures.* Hemisphere Pub. Corp., 1987.

[2] M. Païdoussis, *Fluid-Structure Interactions: Slender Structures and Axial Flow.* Academic Press, 2004.

[3] S. Ersdal and O. M. Faltinsen, "Normal forces on cylinders in near-axial flow," *Journal of Fluids and Structures*, vol. 22, no. 8, pp. 1057–1077, 2006.

[4] M. Hassan, A. Gerber, and H. Omar, "Numerical estimation of fluidelastic instability in tube arrays," *Journal of Pressure Vessel Technology-Transactions of the ASME*, vol. 132, no. 4, 2010.

[5] F. Belanger, M. P. Paidoussis, and E. Delangre, "Time-marching analysis of fluid-coupled systems with large added-mass," *AIAA Journal*, vol. 33, no. 4, pp. 752–757, 1995.

[6] J. De Ridder, J. Degroote, K. Van Tichelen, P. Schuurmans, and J. Vierendeels, "Modal characteristics of a flexible cylinder in turbulent axial flow from numerical simulations," *Journal of Fluids and Structures*, in review.

[7] S. Chen and M. Wambsgan, "Parallel-flow-induced vibration of fuel rods," *Nuclear Engineering and Design*, vol. 18, no. 2, pp. 253–278, 1972.

[8] J. Degroote, K. J. Bathe, and J. Vierendeels, "Performance of a new partitioned procedure versus a monolithic procedure in fluid-structure interaction," *Computers and Structures*, vol. 87, no. 11-12, pp. 793–801, 2009.

[9] T. M. Mulcahy, T. T. Yeh, and A. J. Miskevics, "Turbulence and rod vibrations in an annular region with upstream disturbances," *Journal of Sound and Vibration*, vol. 69, no. 1, pp. 59–69, 1980.